

Platinum(II) Complexes of Dipyridophenazine as Metallointercalators for DNA and Potent Cytotoxic Agents against Carcinoma Cell Lines

Chi-Ming Che,^{*[a]} Mengsu Yang,^{*[b]} Kar-Ho Wong,^[a] Hing-Leung Chan,^[b] and Wing Lam^[b]

Abstract: The synthesis and spectroscopic characterization of a new class of DNA-intercalating platinum(II) complexes, $[\text{Pt}(\text{dppz})(t\text{N}^{\wedge}\text{C})]\text{CF}_3\text{SO}_3$ (dppz = dipyrido[3,2-*a*:2',3'-*c*]phenazine, $t\text{N}^{\wedge}\text{CH} = 4$ -*tert*-butyl-2-phenylpyridine) and $[\text{Pt}(\text{dppz})(\text{L})_2](\text{CF}_3\text{SO}_3)_2$ (L = 1-methylimidazole (Meim-1) or 4-aminopyridine ($\text{NH}_2\text{py-4}$)) are described. All the complexes are photoluminescent in degassed acetonitrile at room temperature. $[\text{Pt}(\text{dppz})(t\text{N}^{\wedge}\text{C})]\text{CF}_3\text{SO}_3$ shows a vibronic structured emission ($\lambda_{\text{max}} = 477$ nm) which is assigned to the intraligand transition (IL) of the C-deprotonated 4-*tert*-butyl-2-phenylpyridine ligand. Both $[\text{Pt}(\text{dppz})(\text{Meim-1})_2]$ -

$(\text{CF}_3\text{SO}_3)_2$ and $[\text{Pt}(\text{dppz})(\text{NH}_2\text{py-4})_2](\text{CF}_3\text{SO}_3)_2$ display a lower energy emission band with λ_{max} at 558 nm, which is originated from a ${}^3\text{MLCT}$ state $[5d(\text{Pt}) \rightarrow \pi^*(\text{dppz})]$. The binding reactions of platinum(II) complexes with double-stranded DNA (dsDNA) were studied by spectroscopic methods and the intrinsic binding constants (K) are $1.1 \times 10^4 - 1.3 \times 10^4 \text{ dm}^3 \text{ mol}^{-1}$. The results of gel electrophoresis and UV melting experiments revealed that

they interact strongly with DNA. In aerated aqueous Tris buffer solution, $[\text{Pt}(\text{dppz})(t\text{N}^{\wedge}\text{C})]\text{CF}_3\text{SO}_3$ is nonemissive. Upon intercalation of $[\text{Pt}(\text{dppz})(t\text{N}^{\wedge}\text{C})]\text{CF}_3\text{SO}_3$ into calf thymus DNA (ctDNA), a low energy emission with $\lambda_{\text{max}} = 650$ nm is developed and this is ascribed to exciplex formation between the excited state of $[\text{Pt}(\text{dppz})(t\text{N}^{\wedge}\text{C})]^+$ with the DNA base pairs. The cytotoxicity of $[\text{Pt}(\text{dppz})(t\text{N}^{\wedge}\text{C})]\text{CF}_3\text{SO}_3$ was compared to that of cisplatin using human carcinoma KB-3-1 and its multi-drug-resistant subclone KB-V1 cell lines, which is 10 and 40 times more potent than cisplatin in the killing of KB-3-1 and KB-V1 cells, respectively.

Keywords: antitumor agents • bioinorganic chemistry • DNA recognition • luminescence • platinum

Introduction

The binding interaction(s) between DNA and transition metal complexes has received intense interest from different perspectives.^[1-3] In general, metal complexes can bind to double-helix DNA noncovalently through electrostatic interaction, groove binding, and/or intercalation. We were particularly interested in the latter which involves insertion of a planar aromatic molecule between two nucleotide base units of the biomolecules. As suggested by Barton and co-workers,^[1e] the DNA π stack is essential for biological electron

transfer reactions to occur over a long distance. In the context of developing new metallointercalators, we were attracted to the work of Barton^[1] and recent findings on the photoluminescence of platinum(II) complexes.^[4,5] Barton and others had reported that octahedral metal complexes containing the dppz ligand (dppz = dipyrido[3,2-*a*:2',3'-*c*]phenazine), in particular that of ruthenium(II), are good metallointercalators and in some instances, act as luminescent probes for biological molecules.^[6-9] However, this class of compounds are coordinatively saturated, and hence the metal atom has difficulty in covalently interacting with nucleic acid. Square-planar platinum(II) complexes of aromatic diimine ligands are a likely remedy to this problem.^[4,10] Usually, they have vacant coordination site(s) at the platinum atom, which is(are) available for substrate binding reactions. Furthermore, this class of compounds displays rich photoluminescent properties, which are sensibly affected by the microenvironment in which the compounds are located.^[4b,d,e,5b,10] A notable example is the luminescent cyclometalated platinum(II) complexes reported by Che and co-workers,^[4d,e] which act as a molecular light switch for calf thymus DNA and sodium dodecyl sulfate (SDS) micelles. We envisaged that platinum(II) complexes containing the dppz ligand have the combined advantages of ruthenium(II) dppz and platinum(II) complexes in the context of DNA binding studies and are potential new metal

[a] Prof. C. M. Che, K. H. Wong
Department of Chemistry
The University of Hong Kong
Pokfulam Road, Hong Kong
Fax: (+852) 2857-1586
E-mail: cmche@hkucc.hku.hk

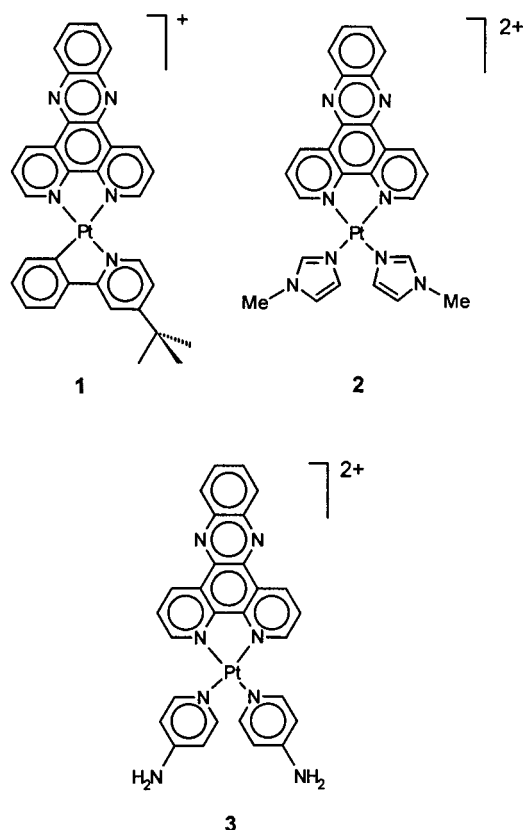
[b] Dr. M. Yang, H. L. Chan, W. Lam
Department of Biology and Chemistry
City University of Hong Kong
83 Tat Chee Avenue, Kowloon, Hong Kong
Fax: (+852) 2788-7406
E-mail: bhmyang@cityu.edu.hk

Supporting information for this article is available on the WWW under <http://www.wiley-vch.de/home/chemistry/> or from the author.

therapeutics. Here, the synthesis, spectroscopic properties, and biological activities of a new class of luminescent platinum(II) complexes bearing the dppz ligand are reported.

Results and Discussion

The titled complexes could be prepared by two methods. For **1**, the $[\text{Pt}(t\text{N}^{\wedge}\text{C})\text{Cl}_2]^-$ precursor was first generated and then allowed to react with dppz to afford the desired product. A different synthetic route was employed for **2** or **3**. $[\text{Pt}(\text{dppz})\text{Cl}_2]$ was the precursor and it underwent chloride



substitution reactions with the nitrogen donor ligands. Recently, the X-ray crystal structure of $[\text{Pt}(\text{dppz})\text{Cl}_2]$ was reported by Kato et al.^[11] Stacking of the $[\text{Pt}(\text{dppz})\text{Cl}_2]$ molecules through platinum–platinum (intermolecular Pt–Pt contacts ca. 3.4 Å) and/or ligand π – π interactions has been revealed by X-ray structure analysis. The reaction between the C-deprotonated 2-phenylpyridine and $[\text{Pt}(\text{dppz})\text{Cl}_2]$ was studied in this work. A deep red product presumably $[\text{Pt}(\text{dppz})(\text{N}^{\wedge}\text{C})]\text{Cl}$ was obtained. This compound has a low solubility in common organic solvents rendering further

studies difficult. For this reason, 4-*tert*-butyl-2-phenylpyridine was used to improve the solubility. Complex **1** is soluble in polar organic solvents rendering spectroscopic characterizations feasible. For complexes **2** and **3**, the imidazole and pyridine ligands can twist with respect to the PtN_4 plane.^[4b, 10d] This structural feature together with the cationic charge support the solubility of **2** and **3** in aqueous solution. The ^1H NMR spectra for **1–3** display the correct number of proton signals and their mass spectra confirm the molecular mass of the corresponding parent complex cation. As shown by ^1H NMR and UV/Vis spectroscopy, complexes **1–3** are stable with regard to solvolysis reaction at room temperature.

Spectroscopic properties: The absorption and emission data for **1–3** are summarized in Table 1. All the complexes show several intense absorption bands at $\lambda < 380$ nm ($\epsilon > 10^4$ dm³ mol⁻¹ cm⁻¹), which are assigned to intraligand transitions (IL) of the dipyridophenazine (**1**, **2**, and **3**) and 4-*tert*-butyl-2-phenylpyridine ligands (**1**). Complex **1** shows a broad and structureless band ranging from 410 to 470 nm ($\epsilon > 10^3$ dm³ mol⁻¹ cm⁻¹). As a similar absorption band is absent in $[\text{Pt}(\text{en})(t\text{N}^{\wedge}\text{C})]^+$ (en = 1,2-diaminoethane),^[12] the assignment of a $(5d)\text{Pt} \rightarrow (\pi^*)t\text{N}^{\wedge}\text{C}^-$ transition is not favored. The absorption spectra of other $[\text{Pt}(\text{N}^{\wedge}\text{N})(t\text{N}^{\wedge}\text{C})]^+$ ($\text{N}^{\wedge}\text{N}$ = bpy or phen) complexes^[12] show a similar band at 400–460 nm, but the λ_{max} value changes with the π^* orbital of the diimine ligands. Hence the broad absorption ranging from 410–470 nm for **1**, which is similarly present in **2** and **3**, is assigned to the $(5d)\text{Pt} \rightarrow (\pi^*)\text{dppz}$ transition. The absorption spectra of the complexes are shown in Figure 1.

At room temperature, a degassed solution of **1**(CF₃SO₃) in acetonitrile gives a vibronic structured emission ($\lambda_{\text{max}} = 477$ nm) upon excitation at 350 nm (Figure 2). The vibrational progression (ca. 1100–1300 cm⁻¹) matches with the skeletal vibrational frequency of the $t\text{N}^{\wedge}\text{C}^-$ ligand. Similar emissions with the same λ_{max} have been recorded with related $[\text{Pt}(\text{N}^{\wedge}\text{N})(t\text{N}^{\wedge}\text{C})]^+$ complexes in acetonitrile, despite the difference in α, α' -diimine ligands.^[12] We infer that the emission at 477 nm originates from a $^3\pi\pi^*$ state of the coordinated $t\text{N}^{\wedge}\text{C}^-$ ligand. The solid-state emission of **1** with λ_{max} at 675 nm is at a lower energy (Figure 2). The large difference in emission energies indicates that the excited states for the solution and solid emissions have different electronic origins. According to previous work,^[13,14] solid-state stacking of platinum(II) complexes affects their photoluminescent properties. Although we were not able to obtain suitable crystals of **1**(CF₃SO₃) for X-ray crystal analysis, $[\text{Pt}(\text{dppz})\text{Cl}_2]$ was found to stack through both platinum–platinum and ligand π – π interactions.^[11] We consider that the $[\text{Pt}(\text{dppz})(t\text{N}^{\wedge}\text{C})]^+$ cation also stacks in solid state and

Table 1. UV/Vis absorption and emission data recorded in acetonitrile at room temperature.

Complex	UV/Vis	Emission
	λ , ^[a] nm (ϵ , ^[b] [dm ³ mol ⁻¹ cm ⁻¹])	λ_{max} , ^[a] nm (τ , ^[c] [μs], Φ_{em} , ^[d])
1 (CF ₃ SO ₃)	280 (69000), 363 (15000), 382 (16000), 410–470 (4500)	477 (2.3, 0.0012)
2 (CF ₃ SO ₃) ₂	280 (71000), 358 (17000) 376 (16000), 400–450 (1200)	558 (74.6, 0.0023)
3 (CF ₃ SO ₃) ₂	280 (89000), 358 (15000) 376 (16000), 400–450 (1100)	558 (79.9, 0.0024)

[a] Error = ± 2 nm. [b] Error = ± 100 dm³ mol⁻¹ cm⁻¹. [c] Error = ± 0.05 μs . [d] Error = ± 0.00005 .

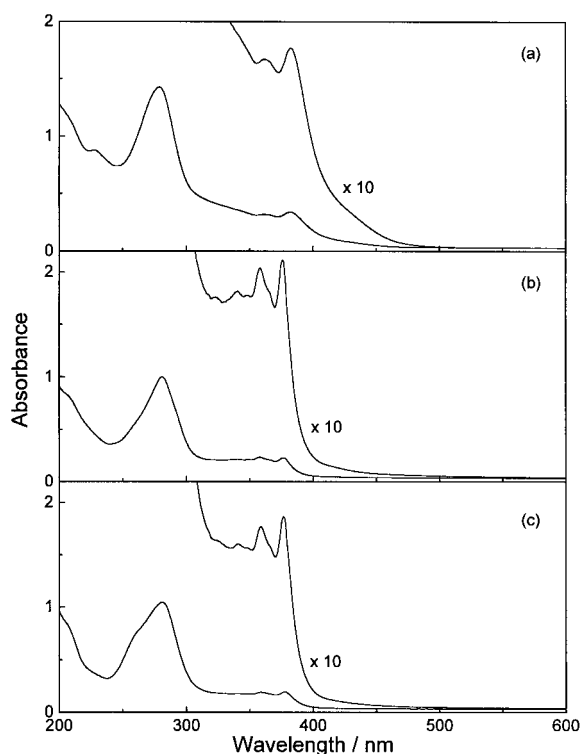


Figure 1. The UV/Vis absorption spectra of a) **1**(CF₃SO₃), b) **2**(CF₃SO₃)₂, and c) **3**(CF₃SO₃)₂ in acetonitrile at room temperature.

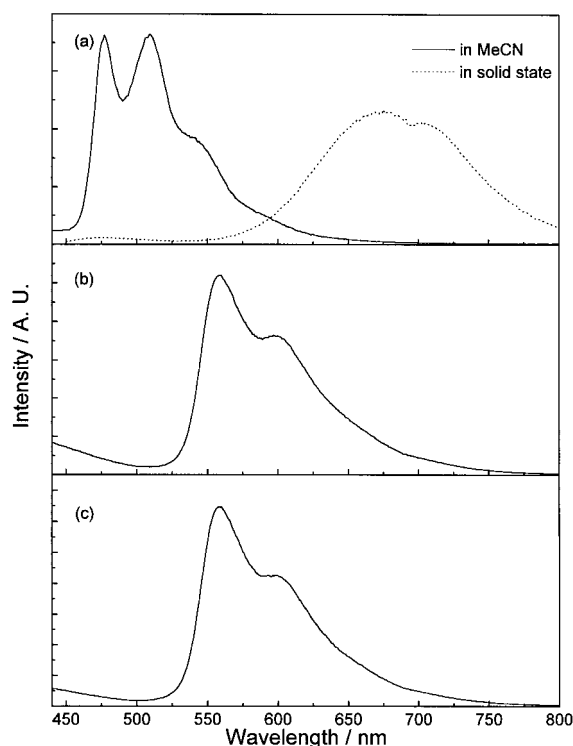


Figure 2. The emission spectra of a 10⁻⁵ mol dm⁻³ acetonitrile solution of a) **1**(CF₃SO₃), b) **2**(CF₃SO₃)₂, and c) **3**(CF₃SO₃)₂ at room temperature. Excitation at 350 nm.

hence a lower energy MMLCT (metal-metal to ligand charge transfer) transition is expected. Indeed, in frozen acetonitrile (77 K), the emission of **1** is distinctly different from that described above. At low complex concentration

(10 μmol dm⁻³), the high energy (474 nm) intraligand (IL) emission of the coordinated tN⁻C⁻ ligand prevailed. Increasing the complex concentration led to a decrease in the 474 nm emission with a concomitant development of a low energy emission at 665 nm. The similarity in energy and band profile of the 665 nm emission to that of the solid-state emission (λ_{max} = 675 nm) at room temperature suggests that the former arises from the interaction between the ground state and excited state of the [Pt(dppz)] moieties. Both Che et al.^[15] and Vogler and Kunkley^[16] had reported that the excimer emission of [Pt(diimine)(CN)₂] occurs at a much lower energy than the intraligand diimine [π → π*] or ³MLCT [(5d)Pt → (π*)diimine] emission. In acetonitrile, complexes **2** and **3** display a vibronic structured emission (λ_{max} = 558 nm) at room temperature (Figure 2). The average vibrational progression is about 1200 cm⁻¹, which matches the frequency of the 'ring-breathing' mode of dipyrrophenazine ligand. For the [Pt(diimine)₂]²⁺ systems, Miskowski and co-workers assigned the intraligand emission of the diimine ligands in glassy solution to occur at around 458 nm.^[13a] Thus the 558 nm emission band of **2** or **3** is assigned to the ³MLCT [(5d)Pt → (π*)dppz] excited state. Interestingly, the metal → dppz emission for Pt^{II} occurs at a higher energy than for Ru^{II}; for example, the ³MLCT emission of [Ru(bpy)₂(dppz)]²⁺ is at 615 nm.^[6] Both **2** and **3** show no solid-state emission at room temperature and 77 K.

DNA binding studies: Absorption and emission titration experiments were performed for complexes **1–3** in the presence of calf thymus DNA. Their absorption spectra in aqueous Tris buffer are similar to that in acetonitrile. The absorption spectral traces for the titration of **1** with ctDNA are depicted in Figure 3. The 350 nm band showed hypochromism upon addition of ctDNA and an isosbestic point at

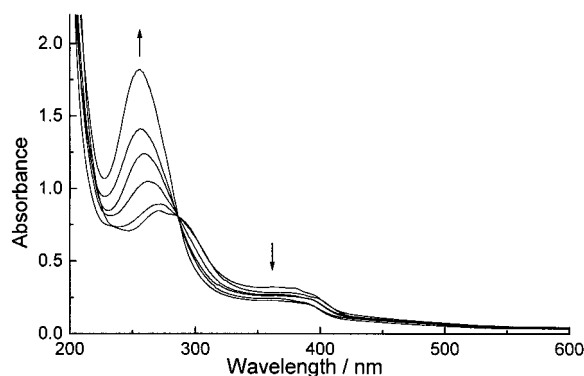


Figure 3. Absorption spectral traces of complex **1**(CF₃SO₃) (20 μmol dm⁻³) in aqueous Tris buffer (5 mmol dm⁻³ Tris, 50 mmol dm⁻³ NaCl, pH 7.2) with increasing ctDNA concentrations: 0, 21, 42, 63, 126, 189 μmol dm⁻³.

286 nm was recorded. The spectral data suggests binding of the metal complex to the biopolymer through a noncovalent intercalative mode.^[17] The intrinsic binding constants *K* were derived from a plot of *D*/Δε_{ap} vs. *D* according to Equation (1)^[18], where *D* is the concentration of DNA in base pairs,

$$D/\Delta\epsilon_{ap} = D/\Delta\epsilon + 1/(\Delta\epsilon \times K) \quad (1)$$

$\Delta\epsilon_{\text{ap}} = |\epsilon_{\text{A}} - \epsilon_{\text{F}}|$ and $\Delta\epsilon = |\epsilon_{\text{B}} - \epsilon_{\text{F}}|$, the apparent extinction coefficient, $\epsilon_{\text{A}} = A_{\text{obs}}/[\text{complex}]$, ϵ_{B} and ϵ_{F} are the extinction coefficients of the bound and free form of the platinum(II) complex, respectively. The slope and y intercept of the linear fit of $D/\Delta\epsilon_{\text{ap}}$ vs. D give $1/\Delta\epsilon$ and $1/(\Delta\epsilon \times K)$, respectively. The binding parameters are listed in Table 2. The intrinsic binding constants K are 1.1×10^4 – $1.3 \times 10^4 \text{ dm}^3 \text{ mol}^{-1}$. These values are comparable to those found in other platinum(II) intercalators.^[4b,10d]

Table 2. The intrinsic binding constant (K) for the Pt^{II} complexes to calf thymus DNA.

Complex	$K [\text{dm}^3 \text{ mol}^{-1}]^{\text{[a]}}$
1 (CF ₃ SO ₃)	1.3×10^4
2 (CF ₃ SO ₃) ₂	1.1×10^4
3 (CF ₃ SO ₃) ₂	1.2×10^4

[a] Error = $\pm 500 \text{ dm}^3 \text{ mol}^{-1}$. The absorbance was monitored at 350 nm for **1**(CF₃SO₃) and at 360 nm for **2**(CF₃SO₃)₂ and **3**(CF₃SO₃)₂.

Square-planar platinum(II) complexes have vacant coordination sites. Their interactions with DNA base pairs would change the local environment around the metal atom, decrease mobility of the complexes, and affect the photoluminescent properties. Indeed, complexes **1–3** are not emissive in aerated Tris buffer solution. However, in the presence of ctDNA, **1** displays an intense photoluminescence with $\lambda_{\text{max}} = 650 \text{ nm}$, as depicted by the emission spectral traces shown in Figure 4. The increase in emission intensity on addition of ctDNA is similar to that found with the cyclometalated platinum(II) complexes.^[4d] This is ascribed to a decrease in complex–solvent interaction and reduced mobility of the complex. However, the λ_{max} of the emission developed by addition of DNA to **1** deserves further discussion. As mentioned in the previous section, the ³MLCT [(5d)Pt → (π*)dppz] emission of mononuclear Pt^{II} dppz complexes is at 558 nm, which is at a higher energy than the 650 nm emission. Indeed, the latter is comparable in energy to the excimer emission of complex **1** with λ_{max} at 665 nm. But since only one [Pt(dppz)(tN[∧]C)]⁺ is likely to be intercalated between two DNA base pairs, the possibility of having an excimer emission of two [Pt(dppz)(tN[∧]C)]⁺ ions is not favored. In such a case, we ascribe the 650 nm emission to

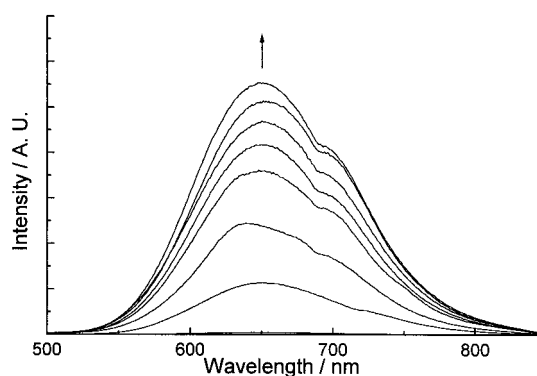


Figure 4. Emission spectral traces of complex **1**(CF₃SO₃) (20 $\mu\text{mol dm}^{-3}$) in aqueous Tris buffer (5 mmol dm^{-3} Tris, 50 mmol dm^{-3} NaCl, pH 7.2) with increasing increasing ctDNA concentrations: 0, 21, 42, 63, 84, 105, 126, 189 $\mu\text{mol dm}^{-3}$.

exciplex formation between the DNA base pair and [Pt(dppz)(tN[∧]C)]⁺ in the excited state (Figure 5). Indeed, Balzani and co-workers had reported a similar kind of exciplex emission to occur at about 600 nm for the [Pt(bpy)(NH₃)₂]²⁺–dibenzo[30]crown-10 adduct.^[19] Complexes **2** and **3** show no photoluminescence even in the presence of ctDNA in aerated Tris buffer. For the “**1** + DNA” system, a plot of I/I_0 vs. [DNA]/[complex], where I and I_0 are the emission intensities in the presence and absence of ctDNA, respectively, indicates that the emission intensity is enhanced by 140 times at a [DNA]:[complex] ratio of 14:1 (Figure 6). The emission titration data were analyzed with the McGhee–von Hippel equation [Eq. (2)],^[20] where $r = (C_T - C_F)/[\text{DNA}]$ and $C_F = C_T[(I/I_0) - P]/(1 - P)$. C_T is the

$$r/C_F = K(1 - nr)\{(1 - nr)/[1 - (n - 1)r]\}^{n-1} \quad (2)$$

total concentration of the complex, C_F is the concentration of the free complex, n is the binding site size in base pairs, and P is given by the y intercept of the plot of I/I_0 vs. $1/[\text{DNA}]$. Fitting the experimental data gave $K = 1.0 \times 10^4 \text{ mol}^{-1} \text{ dm}^3$, $n = 1$. While the intrinsic binding constant determined by emission titration experiments closely matches with that determined by absorption titration experiment ($1.3 \times 10^4 \text{ mol}^{-1} \text{ dm}^3$), the binding site size of **1** is too small to

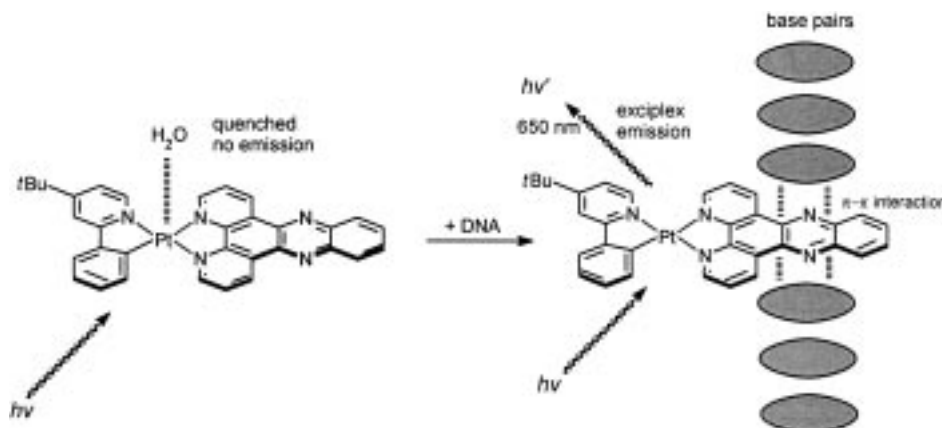


Figure 5. Schematic illustration of the interaction between complex cation **1** and DNA.

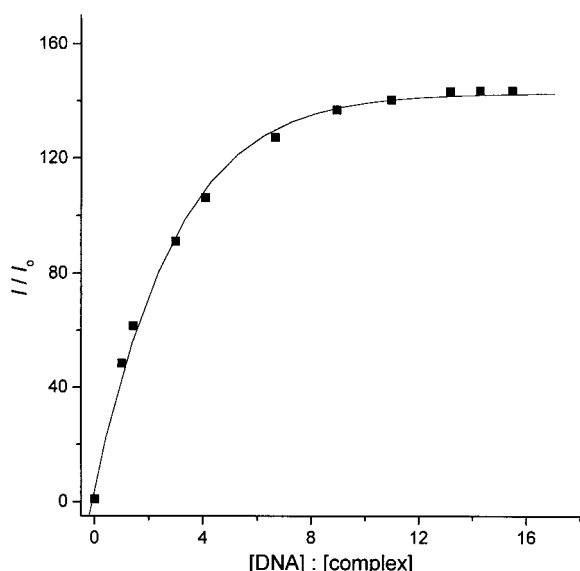


Figure 6. A plot of I/I_0 vs. $[DNA]/[complex]$ for $\mathbf{1}(\text{CF}_3\text{SO}_3)$. The emission intensity was monitored at 650 nm.

account for the neighbor exclusion principle. The possibility that some of the complex molecules bind to DNA by alternate modes cannot be ruled out.

DNA intercalation requires changes in sugar–phosphate chain torsion angles for separation of adjacent base-pairs to allow insertion of the complex, which causes extension of the DNA duplex, local unwinding of the base-pairs, and other conformational distortions in the DNA backbone. To gain insight into the binding mode of the complexes, the structural changes of DNA associated with the bindings were investigated by gel electrophoresis which is sensitive to DNA conformation, as well as by DNA melting experiments which are sensitive to the unwinding of base pairs. Figure 7 shows the typical results of polyacrylamide gel electrophoresis of a 33-bp DNA in the presence of $\mathbf{1}$. Smearing and tailing of the

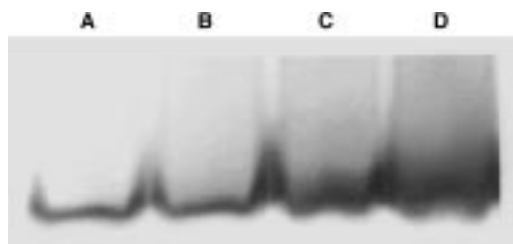


Figure 7. 20% polyacrylamide gel showing the results of electrophoresis of a 33-bp DNA ($165 \mu\text{mol dm}^{-3} \text{bp}^{-1}$) in the presence of $\mathbf{1}(\text{CF}_3\text{SO}_3)$ ($\mu\text{mol dm}^{-3}$) at various concentrations: A) 0, B) 1, C) 5, D) 25.

DNA bands were observed with increasing complex concentration. Since the mobility of DNA through a gel strongly depends on the length of DNA molecules (the frictional force on DNA exerted by the gel matrix is proportional to the length of DNA molecules), the results indicate a lengthening of the DNA due to its interaction with the complex. The binding of $\mathbf{1}$ to DNA is nonspecific towards either GC or AT sites, as shown by the increasing conformational polymorphism of DNA with increasing complex concentration. Similar

results were observed using a plasmid DNA (pBR322) and 1% agarose gel. These observations indicate that the binding of $\mathbf{1}$ to dsDNA is intercalative in nature and is not sequence specific. Additional evidence for intercalation was obtained by the restriction cleavage assay. As shown in Figure 8, a plasmid DNA (pDR2, 10.7-kb) can be readily cleaved by endonuclease EcoR I into five fragments (Lane B). Intercalation of $\mathbf{1}$ into pDR2 leads to a conformational change of the DNA, which cannot be recognized by EcoR I. As a result, no cleavage of pDR2 was observed.

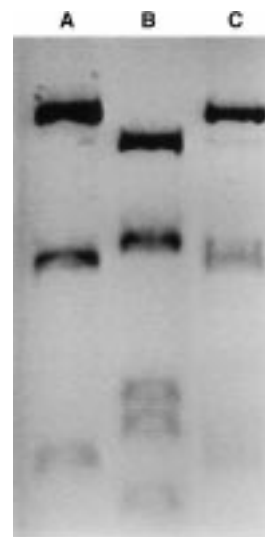


Figure 8. 0.8% agarose gel showing the results of electrophoresis of a plasmid DNA pDR2. A) negative control containing pDR2 ($21 \text{ nmol dm}^{-3} \text{bp}^{-1}$) only; B) pDR2 ($21 \text{ nmol dm}^{-3} \text{bp}^{-1}$) digested with restriction endonuclease EcoR I; C) pDR2 could not be digested by EcoR I in the presence of $\mathbf{1}(\text{CF}_3\text{SO}_3)$ ($200 \mu\text{mol dm}^{-3}$).

Melting of DNA is a phenomenon observed when double-stranded DNA molecules are heated and separated into two single strands; it occurs due to disruption of the intermolecular forces such as π – π stacking and hydrogen bonding interactions between the DNA base pairs. The DNA melting experiments reveal that T_m of the 33-bp DNA ($1.65 \times 10^{-5} \text{ mol dm}^{-3} \text{bp}^{-1}$) was 88.5 and 69.5 °C in the absence and presence of $\mathbf{1}$ ($1.00 \times 10^{-5} \text{ mol dm}^{-3}$), respectively. The reduction in T_m indicates a reduced affinity of the DNA double helix due to the unwinding of the DNA helix and suggests unstacking of the DNA bases upon intercalation of the complex.

Cytotoxicity: The biological activity of $\mathbf{1}$ was studied by its in vitro cytotoxicity against KB-3-1 and KB-V1 cell lines. The former is a sensitive human epidermal carcinoma cell line, while the latter is a multidrug-resistant subclone. The cytotoxicities of $\mathbf{1}$ and the clinically used anticancer drug, cisplatin (*cis*-diamminedichloroplatinum(II)), are listed in Table 3. It is known that cisplatin undergoes solvolysis of the Pt–Cl bond to give reactive Pt–OH₂ species, which crosslinks with DNA and exerts its antitumor activity by inhibition of DNA replication. On the other hand, $\mathbf{1}$ is substitutionally inert and the coordinated chelated ligands are

Table 3. Cytotoxicities of complex **1**(CF₃SO₃) and cisplatin in human carcinoma KB-3-1 cells and its multidrug-resistant subclone KB-V1 cells.

Complex	D_m [μM] ^[a]		D_m ratio KB-V1/KB-3-1
	KB-3-1	KB-V1	
1 (CF ₃ SO ₃)	1.7 ± 0.5	1.0 ± 0.5	0.59
cisplatin	22.1 ± 3.6	39.1 ± 1.7	1.77

[a] Median dose values (D_m) were determined from plots of median effects: $\log(F_a/F_u) = \log(D/D_m)^m$ and is equivalent to the LD₅₀, where F_a and F_u are the fraction affected and unaffected by dose (D), respectively, and m is a coefficient of the sigmoidicity of the dose-effect curve. Values are mean values ± SEM.

stable with regard to solvolysis reactions. However, the results showed that **1** is a potent cytotoxic agent in both KB-3-1 and KB-V-1 cell lines. In comparison with cisplatin, it is 10 and 40 times more toxic towards both KB-3-1 and KB-V-1 cells, respectively. The ratio of the cytotoxicities for the two cell lines ($D_m(\text{KB-V1}):D_m(\text{KB-3-1})$) was found to be 0.6 and 1.8 for **1** and cisplatin, respectively. According to this ratio, the complex is more efficient in killing of the multidrug-resistant KB-V1 cells than the sensitive KB-3-1 cells, as judged by the paired t-test. These findings imply that **1** is not only a potent cytotoxic agent against different human carcinoma cell lines but also confers certain advantages in overcoming multidrug resistance in these cell lines. Because of the substitutional inertness of the chelated dppz or *tN^A*C⁻ ligand, **1** is unlikely to crosslink DNA in a similar fashion as cisplatin does. Rather, it could be the intercalation that inhibits the DNA replication. Of course, the possibility that the cytotoxicity is due to inhibition of cellular functions other than DNA replication cannot be ruled out.

Experimental Section

All starting materials were used as received, and the solvents were purified according to literature methods.^[21] 4-*tert*-Butyl-2-phenylpyridine was prepared by the procedure from Vogel,^[22] dipyrrodo[3,2-*a*:2',3'-*c*]phenazine,^[23] Bu₄N[Pt(*tN^A*C)Cl₂],^[24] and [Pt(dppz)Cl₂]^[11] were prepared according to published methods. Calf thymus DNA (type I) was purchased from Sigma Chemical Co. and purified by phenol extraction as described in literature.^[25]

¹H NMR spectra were recorded on a DPX-300 Bruker FT-NMR spectrometer with chemical shift (in ppm) relative to tetramethylsilane. FAB mass spectra were recorded on a Finnigan MAT 95 Mass Spectrometer using 3-nitrobenzyl alcohol (NBA) as matrix. UV/Vis spectra were recorded on a Perkin Elmer Lambda 19 UV/vis spectrophotometer. Emission spectra were obtained on a SPEX Fluorolog-2 Model F11 fluorescence spectrophotometer. Elemental analysis was performed on a Carlo Erba 1106 elemental analyzer at the Institute of Chemistry, Chinese Academy of Sciences. All spectroscopic titrations were carried out in aerated aqueous Tris buffer (5 mmol dm⁻³ Tris, 50 mmol dm⁻³ NaCl, pH 7.2).

Two complementary 33-mer oligonucleotides (5'-GCTCCCCTTCTTG-CGGAGATTCTCTTCCTCTG; 5'-CAGAGGAAGAGAATCTCCG-CAAGAAAGGGGAGC) were synthesized (Gene Assembler Special, Pharmacia) and annealed at 95 °C to prepare a well-defined 33-bp dsDNA. The DNA (0.17 mmol dm⁻³ bp⁻¹) was mixed with various concentrations (0–1.0 mmol dm⁻³) of the platinum complex and the mixtures were analyzed by gel electrophoresis (D GENE System with Power Pac 300 power supply, Bio-Rad) using 20% polyacrylamide gel and 1 × Tris-borate electrophoresis (TBE) buffer.

Digestion of a 10.7-kb plasmid DNA (pDR2, Clontech) with the restriction enzyme EcoR I (New England Biolabs) was carried out by mixing the DNA (21 nmol dm⁻³ bp⁻¹) in 1 × EcoR I digestion buffer (New England Biolabs)

with EcoR I (1 unit μL^{-1}), followed by incubation at 37 °C for one hour. For the effect of complex **1**, the DNA solution was first mixed with the complex (200 $\mu\text{mol dm}^{-3}$) at room temperature for 5 min before addition of EcoR I. The DNA samples were analyzed by running a 0.8% agarose gel electrophoresis.

UV melting experiments were carried out in deionized water solution using a UV/Visible spectrophotometer (Lambda 19, Perkin-Elmer) equipped with a temperature programmer (PTP-6, Peltier). The absorbance at 260 nm was monitored for either the same 33-bp DNA (1.65×10^{-5} mol dm⁻³ bp⁻¹) or a mixture of the DNA (1.65×10^{-5} mol dm⁻³ bp⁻¹) with the complex (1.00×10^{-5} mol dm⁻³). The UV melting temperature (T_m) is defined as the temperature at which half the helical structure is lost. The parental KB-3-1 cell line and the multidrug-resistant KB-V1 cell line derived from KB-3-1 cells by a series of stepwise selections in vinblastin were generously provided by Dr. Michael Gottesman, National Institute of Health, Bethesda.^[26, 27] Cells were grown as monolayers in minimal essential medium (MEM-Eagle, Sigma) supplemented with 10% fetal calf serum (FCS, Gibco) and 1% Sigma A-7292 Antibiotic and Antimycotic Solution. KB-V1 cells were maintained in the presence of 1 $\mu\text{g mL}^{-1}$ vinblastin. For the measurement of cytotoxicity, the complex was dissolved in spectroscopic grade dimethylsulphoxide. The dose response curves of drug effects on cell survival were determined by the tetrazolium salt MTT assay.^[28] The median dose value (D_m) was determined from plots of median effects^[29,30] and is equivalent to the LD₅₀.

[Pt(dppz)(*tN^A*C)]CF₃SO₃ [1**(CF₃SO₃)]:** A mixture of Bu₄N[Pt(*tN^A*C)Cl₂] (0.50 g, 0.70 mmol) and AgCF₃SO₃ (0.36 g, 1.40 mmol) in ethanol (50 mL) was refluxed for 4 h. The AgCl formed was filtered through celite and dppz (0.20 g, 0.70 mmol) was added to the filtrate. The resulting mixture was refluxed for 12 h and its volume was reduced to 5 mL. Addition of diethyl ether gave a yellow precipitate, which was filtered and washed with diethyl ether (2 × 5 mL). The crude product was recrystallized from acetonitrile. Yield 0.29 g, 49%; elemental analysis calcd (%) for C₂₄H₂₆N₃F₃O₃SPT (836.75): C 48.80, H 3.13, N 8.37; found: C 48.76, H 3.10, N 8.34; ¹H NMR (300 MHz, CD₃CN, 25 °C, TMS): δ = 9.32 (d, 1H), 9.24 (d, 1H), 9.19 (d, 1H), 9.03 (d, 1H), 8.25 (m, 3H), 8.18 (m, 3H), 7.86 (dd, 1H), 7.24 (d, 1H), 6.95 (s, 1H), 6.71 (d, 2H), 6.44 (m, 1H), 6.18 (d, 1H), 1.41 (s, 9H); MS-FAB: m/z (%): 687 (100) [M^+].

[Pt(dppz)(Meim-1)₂](CF₃SO₃)₂ [2**(CF₃SO₃)₂]:** A mixture of [Pt(dppz)Cl₂] (0.30 g, 0.55 mmol) and excess 1-methylimidazole (0.90 mL, 10 mmol) in absolute ethanol (50 mL) was refluxed for 24 h. A clear dark brown solution was obtained and excess LiCF₃SO₃ was added to give a green precipitate, which was filtered and washed with diethyl ether (2 × 5 mL). The crude product was recrystallized from acetonitrile. Yield 0.25 g, 48%; elemental analysis calcd (%) for C₂₈H₂₂N₈F₆O₆S₂Pt (939.73): C 35.78, H 2.36, N 11.92; found: C 35.76, H 2.33, N 11.95; ¹H NMR (300 MHz, [D₆]DMSO, 25 °C, TMS): δ = 9.92 (d, 2H), 8.71 (s, 2H), 8.51 (m, 2H), 8.38 (m, 2H), 8.27 (m, 4H), 7.70 (s, 2H), 7.56 (s, 2H), 3.89 (s, 6H); MS-FAB: m/z (%): 790 (20) [$M^{2+} + \text{CF}_3\text{SO}_3^-$], 641 (40) [M^{2+}], 559 (100) [C₂₂H₁₆N₆Pt⁺].

[Pt(dppz)(NH₂py-4)₂](CF₃SO₃)₂ [3**(CF₃SO₃)₂]:** The procedure was similar to that for **2**(CF₃SO₃)₂, except 4-aminopyridine (1.03 g, 10 mmol) was used. Yield 0.23 g, 43%; elemental analysis calcd (%) for C₃₀H₂₂N₈F₆O₆S₂Pt (963.75): C 37.39, H 2.30, N 11.62; found: C 37.42, H 2.33, N 11.65; ¹H NMR (300 MHz, [D₆]DMSO, 25 °C, TMS): δ = 9.92 (d, 2H), 8.54 (m, 2H), 8.38 (m, 6H), 8.26 (m, 4H), 7.40 (s, 4H), 6.75 (d, 4H); MS-FAB: m/z (%): 814 (20) [$M^{2+} + \text{CF}_3\text{SO}_3^-$], 665 (40) [M^{2+}], 571 (100) [C₂₃H₁₆N₆Pt⁺].

Acknowledgments

We are grateful to the supports from The University of Hong Kong and the Hong Kong Research Grants Council.

- [1] a) A. M. Pyle, J. K. Barton, *Prog. Inorg. Chem.* **1990**, *38*, 413–475; b) C. S. Chow, J. K. Barton, *Methods Enzymol.* **1992**, *212*, 219–242; c) C. J. Murphy, M. R. Arkin, Y. Jenkins, N. D. Ghatlia, S. H. Bossmann, N. J. Turro, J. K. Barton, *Science* **1993**, *262*, 1025–1029; d) P. J. Dandliker, R. E. Holmlin, J. K. Barton, *Science* **1997**, *275*, 1465–1468; e) R. E. Holmlin, P. J. Dandliker, J. K. Barton, *Angew.*

- Chem.* **1997**, *109*, 2830–2848; *Angew. Chem. Int. Ed. Engl.* **1997**, *36*, 2714–2730.
- [2] D. S. Sigman, A. Mazumder, D. M. Perrin, *Chem. Rev.* **1993**, *93*, 2295–2316.
- [3] V. Balzani, R. Ballardini, *Photochem. Photobiol.* **1990**, *52*, 409–416.
- [4] a) C. W. Chan, L. K. Cheng, C. M. Che, *Coord. Chem. Rev.* **1994**, *132*, 87–97; b) H. Q. Liu, S. M. Peng, C. M. Che, *J. Chem. Soc. Chem. Commun.* **1995**, 509–510; c) T. C. Cheung, K. K. Cheung, S. M. Peng, C. M. Che, *J. Chem. Soc. Dalton Trans.* **1996**, 1645–1651; d) H. Q. Liu, T. C. Cheung, C. M. Che, *Chem. Commun.* **1996**, 1039–1040; e) L. Z. Wu, T. C. Cheung, C. M. Che, K. K. Cheung, M. H. W. Lam, *Chem. Commun.* **1998**, 1127–1128.
- [5] a) J. Zuleta, M. S. Burberry, R. Eisenberg, *Coord. Chem. Rev.* **1990**, *97*, 47–64; b) C. S. Peyratout, T. K. Aldridge, D. K. Crites, D. R. McMillin, *Inorg. Chem.* **1995**, *34*, 4484–4489; c) S. D. Cummings, R. Eisenberg, *J. Am. Chem. Soc.* **1996**, *118*, 1949–1960; d) R. Büchner, J. S. Field, R. J. Haines, C. T. Cunningham, D. R. McMillin, *Inorg. Chem.* **1997**, *36*, 3952–3956.
- [6] a) A. E. Friedman, J. C. Chambron, J. -P. Sauvage, N. J. Turro, J. K. Barton, *J. Am. Chem. Soc.* **1990**, *112*, 4960–4962; b) R. M. Hartshorn, J. K. Barton, *J. Am. Chem. Soc.* **1992**, *114*, 5919–5925; c) Y. J. Jenkins, J. K. Barton, *J. Am. Chem. Soc.* **1992**, *114*, 8736–8738; d) C. Turro, S. H. Bossmann, Y. Jenkind, J. K. Barton, N. J. Turro, *J. Am. Chem. Soc.* **1995**, *117*, 9026–9032.
- [7] a) C. Hiort, P. Lincoln, B. Nordén, *J. Am. Chem. Soc.* **1993**, *115*, 3448–3454; b) I. Haq, P. Lincoln, D. C. Suh, B. Nordén, B. Z. Chowdhry, J. B. Chaires, *J. Am. Chem. Soc.* **1995**, *117*, 4788–4796; c) P. Lincoln, A. Broo, B. Nordén, *J. Am. Chem. Soc.* **1996**, *118*, 2644–2653; d) S. D. Choi, M. S. Kim, S. K. Kim, P. Lincoln, E. Tuite, B. Nordén, *Biochemistry* **1997**, *36*, 214–223.
- [8] a) C. G. Coates, L. Jacquet, J. J. McGarvey, S. E. J. Bell, A. H. R. Alobaidi, J. M. Kelly, *Chem. Commun.* **1996**, 35–36; b) C. G. Coates, L. Jacquet, J. J. McGarvey, S. E. J. Bell, A. H. R. Alobaidi, J. M. Kelly, *J. Am. Chem. Soc.* **1997**, *119*, 7130–7136.
- [9] a) H. D. Stoeffler, N. B. Thornton, S. I. Temkin, K. S. Schanze, *J. Am. Chem. Soc.* **1995**, *117*, 7119–7128; b) V. W. W. Yam, K. K. W. Lo, K. K. Cheung, R. Y. C. Kong, *J. Chem. Soc. Dalton Trans.* **1997**, 2067–2072; c) S. Arounaguini, B. G. Maiya, *Inorg. Chem.* **1996**, *35*, 4267–4270.
- [10] a) W. I. Sundquist, S. J. Lippard, *Coord. Chem. Rev.* **1990**, *100*, 293–322; b) G. Arena, M. Scolaro, R. F. Pasternack, R. Romeo, *Inorg. Chem.* **1995**, *34*, 2994–3002; c) M. Cusumano, M. L. Di Pietro, A. Giannetto, *Chem. Commun.* **1996**, 2527–2528; d) M. Cusumano, M. L. Di Pietro, A. Giannetto, F. Nicolò, E. Rotondo, *Inorg. Chem.* **1998**, *37*, 563–568.
- [11] M. Kato, C. Kosuge, S. Yano, M. Kimura, *Acta Crystallogr. Sect. C* **1998**, *54*, 621–623.
- [12] [Pt(en)(tN⁺C)]CF₃SO₃, [Pt(bpy)(tN⁺C)]CF₃SO₃, and [Pt(phen)(tN⁺C)]CF₃SO₃ were synthesized in order to assign the electronic origin of the excited state of complex **1**. The synthetic procedure, full characterization data, UV/Vis and emission spectroscopic data are available in the Supporting Information.
- [13] a) V. M. Miskowski, V. H. Houlding, *Inorg. Chem.* **1989**, *28*, 1529–1533; b) V. M. Miskowski, V. H. Houlding, *Inorg. Chem.* **1991**, *30*, 4446–4452; c) V. H. Houlding, V. M. Miskowski, *Coord. Chem. Rev.* **1991**, *111*, 145–152; d) V. M. Miskowski, V. H. Houlding, C. M. Che, Y. Wang, *Inorg. Chem.* **1993**, *32*, 2518–2524.
- [14] W. B. Connick, L. M. Henling, R. E. Marsh, H. B. Gray, *Inorg. Chem.* **1996**, *35*, 6261–6265.
- [15] K. T. Wan, C. M. Che, K. C. Cho, *J. Chem. Soc. Dalton Trans.* **1991**, 1077–1080.
- [16] H. Kunkely, A. Vogler, *J. Am. Chem. Soc.* **1990**, *112*, 5625–5627.
- [17] V. A. Bloomfield, D. M. Crothers, I. Tinoco, Jr., in *Physical Chemistry of Nucleic Acids*, Harper and Row, New York, **1974**, p432.
- [18] A. Wolfte, G. H. Shimer, Jr., T. Meehan, *Biochemistry* **1987**, *26*, 6392–6396.
- [19] a) R. Ballardini, M. T. Gandolfi, V. Balzani, F. H. Kohnke, J. F. Stoddart, *Angew. Chem.* **1988**, *100*, 712–714; *Angew. Chem. Int. Ed. Engl.* **1988**, *27*, 692–694; b) R. Ballardini, M. T. Gandolfi, L. Prodi, M. Ciano, V. Balzani, F. H. Kohnke, H. Shahriari-Zavareh, N. Spencer, J. F. Stoddart, *J. Am. Chem. Soc.* **1989**, *111*, 7072–7078.
- [20] C. V. Kumar, E. H. Asuncion, *J. Am. Chem. Soc.* **1993**, *115*, 8547–8553.
- [21] D. D. Perrin, W. L. F. Armarego, D. R. Perrin in *Purification of Laboratory Chemicals*, 2nd ed., Pergamon, Oxford, **1980**.
- [22] E. Vogel in *Textbook of Practical Organic Chemistry*, 5th ed., ELBS, **1989**.
- [23] M. Yamada, Y. Tanaka, Y. Yoshimoto, S. Kuroda, I. Shimao, *Bull. Chem. Soc. Jpn.* **1992**, *65*, 1006–1011.
- [24] P.-I. Kvam, J. Songstad, *Acta Chem. Scand.* **1995**, *49*, 313–324.
- [25] T. Maniatis, E. F. Fritsch, J. Sambrook in *Molecular Cloning: A Laboratory Manual*, Cold Spring Harbor Laboratory, New York, **1982**, p458.
- [26] S. I. Akiyama, A. Fojo, J. A. Hanover, I. Pastan, M. M. Gottesman, *Somatic Cell Mol. Genet.* **1985**, *11*, 117–126.
- [27] D. W. Shen, C. Carderalli, M. Cornwell, M. M. Gottesman, J. Hwang, S. Ishii, I. Pastan, N. D. Richert, *J. Biol. Chem.* **1986**, *261*, 7762–7770.
- [28] T. Mosmann, *J. Immun. Meth.* **1983**, *65*, 55–63.
- [29] T. C. Chou, P. Talalay, *Adv. Enzyme Regul.* **1984**, *22*, 27–55.
- [30] T. C. Chou, D. Rideout, J. Chou, J. R. Bertino in *Encyclopedia of Human Biology*, Vol. 2, Academic Press, San Diego, **1991**, p371.

Received: January 12, 1999

Revised version: May 3, 1999 [F1535]